Heterojunction Bipolar Transistors for Microwave and Millimeter-wave Integrated Circuits

P. M. ASBECK, MEMBER, IEEE, M. F. CHANG, MEMBER, IEEE, K.-C. WANG, D. L. MILLER, G. J. SULLIVAN, N. H. SHENG, MEMBER, IEEE, E. SOVERO, MEMBER, IEEE, AND J. A. HIGGINS, SENIOR MEMBER, IEEE

Abstract —**This paper reviews the present status of GaAlAs/GaAs HBT technology and projects the impact of these devices on microwave and millimeter-wave integrated circuits. Devices with f_{max} above 120 GHz are described. Differential amplifiers are shown to have offset voltages with standard deviation below 2 mV and voltage gain as high as 200 per stage. Breakdown voltages (BV_{CB0}) above 20 V are demonstrated. Frequency dividers operating above 20 GHz are described.**

I. INTRODUCTION

PRIOR TO THE advent of GaAs technology, microwave transistors were predominantly bipolar devices fabricated with Si. During the past 15 years, FET's based on GaAs offering improved high-frequency performance have been developed and widely applied in microwave systems. Most recently, research efforts have led to the demonstration of heterojunction bipolar transistors (HBT's) [1] based on GaAs and other III–V compounds. These new devices offer the prospect of obtaining performance features similar to those of Si bipolar transistors translated to substantially higher frequency. This paper reviews the status of HBT technology development and the characteristics of HBT's fabricated at present. It subsequently discusses the prospects for application of these HBT's in microwave and millimeter-wave IC's, with emphasis on the areas where the unique characteristics of HBT's may lead to performance improvements over GaAs FET's.

A variety of III–V's are suitable for high-performance HBT's. This paper is primarily concerned with GaAlAs/GaAs heterostructures. Outstanding results are also emerging with InP or InAlAs/InGaAs lattice-matched to InP, which will not be discussed [2]. Most attention is focused here on n-p-n transistors. Recently, p-n-p HBT's have been shown to be capable of attaining high performance as well [3].

While GaAlAs/GaAs HBT research is being conducted at over 20 laboratories around the world, the majority of the examples presented are from the authors' laboratory (Rockwell International).

Manuscript received May 15, 1987; revised August 21, 1987. The Rockwell portions of this work were partially supported by DARPA and were monitored by the Office of Naval Research.

The authors are with the Rockwell International Science Center, Thousand Oaks, CA 91360.

IEEE Log Number 8717398.

II. HBT STRUCTURE

Fig. 1 illustrates a representative n-p-n HBT cross section; its corresponding band diagram along the direction of electron travel is shown in Fig. 2. Table I details the epitaxial layers that form the structure. The HBT derives its name from the use of semiconductors of varying compositions. The bandgap of the emitter material (typically $Ga_{0.75}Al_{0.25}As$) is wider than that of the base material (by 0.33 eV in the typical case). Material composition may also be intentionally varied continuously in the base region, for example, to build in a drift field to propel electrons across this region. The composition of the collector may correspond to GaAs or to the higher bandgap material to reduce charge storage during transistor saturation, and to reduce offset voltages.

The structure of the HBT leads to a number of inherent advantages over Si bipolars, including the following [1]:

- Due to the wide bandgap emitter, a much higher base doping concentration can be used, decreasing base resistance. The emitter injection efficiency is not impaired because the barrier for the hole injection at the base emitter junction is larger than the corresponding barrier for electron injection.
- Emitter doping can be lowered, and minority carrier storage in the emitter can be made negligible, reducing base–emitter capacitance.
- High electron mobility, built-in drift fields and velocity overshoot combine to reduce electron transit times.
- Semi-insulating substrates help reduce pad parasitics and allow convenient integration of devices.
- Output conductance is reduced, and high injection effects are made negligible due to the high base doping.

In comparison with FET's, HBT's also have many intrinsic advantages:

- The key distances that govern electron transit time are established by epitaxial growth, not by lithography, which allows high f_t with modest processing require-

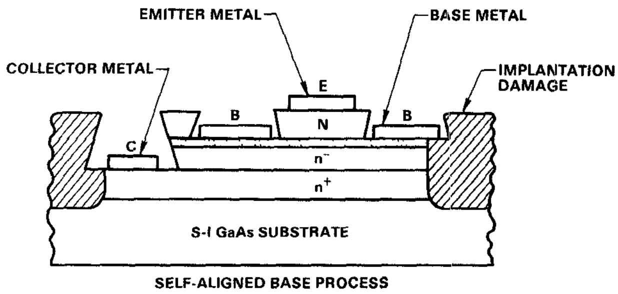

Fig. 1. Representative HBT cross section.

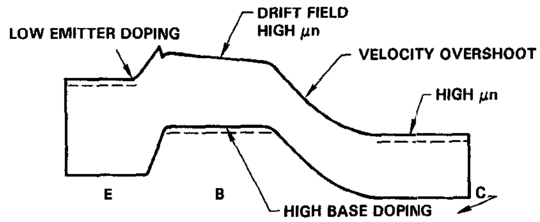

Fig. 2. Schematic HBT energy band diagram. Majority carrier Fermi levels in the quasi-neutral regions are indicated.

TABLE I
REPRESENTATIVE HBT LAYER STRUCTURE

Device Layer	AlAs Mol Fraction	Thickness (Å)	Doping (cm^{-3})
n^+ Cap	0	500	1×10^{19}
N Emitter	0–0.25–0	2000	5×10^{17}
p^+ Base	0	700	10^{19}–10^{20}
n^- Collector	0	7000	3–6×10^{16}
n^+ Subcollector	0	6000	5×10^{18}
Semi-Insulating GaAs Substrate			

ments. High performance may be obtained without submicrometer lithography.

- The entire emitter area conducts current, leading to high current handling capability per unit chip area.
- High transconductance results from the direct control over current flow by the input voltage, as is typical of bipolars (resulting in exponential input–output characteristics).
- The "control region" of the device, the base-emitter junction, is very well shielded from the output voltage, leading to low output conductance g_o; taken together with the high transconductance g_m, enormous values of voltage amplification factor g_m/g_o are attainable.
- Breakdown voltage is directly controllable by the epitaxial structure of the device.
- The threshold voltage for output current flow is governed by the built-in potential of the base–emitter junction, leading to well-matched characteristics.
- The device is well shielded from traps in the bulk and surface regions, contributing to low $1/f$ noise, and absence of trap-induced frequency dependence of output resistance or current lag phenomena.

Experimental verification of each of these advantages is presented in the results below.

When compared with FET's, HBT's have several disadvantageous features as well. The principal ones are:

- Charge storage when operated in saturation conditions (even with wide bandgap collectors).
- Finite current gain at dc due to electron–hole recombination.
- The need to access several different layers of the vertical structure, which can lead to nonplanar structures in some circumstances. This nonplanarity complicates device processing, although it does not preclude monolithic integration of HBT's.

III. Device Technology

Most of the HBT work to date has employed GaAlAs/GaAs layer structures grown by molecular beam epitaxy (MBE). Attention is also being given to the use of metallorganic chemical vapor deposition (MOCVD) as the prospect of volume manufacturing nears. The development of these advanced epitaxial growth techniques has been an essential factor for the development of HBT's (as well as for that of heterostructure FET's). Moreover, continued advancement in these growth technologies is important for the future of the devices. The widespread use of heterostructure bipolar transistors and FET's is dependent on the ready availability of epitaxially grown III–V wafers with the necessary uniformity, reproducibility, low defect density, and low cost.

Control over layer thickness and doping on the order of 10 percent is needed for reproducible HBT characteristics, and interface abruptness must be on the order of 100 Å or better. Material purity is of little concern (background doping concentration below 10^{16} cm^{-3} is adequate). These requirements are less severe than in the case of heterostructure FET's.

HBT's typically have base doping of 5×10^{18} cm^{-3} or above. Recently, transistors with very high base doping (1–2×10^{20} cm^{-3}) have been demonstrated [4], [5], leading to base sheet resistances in the range 100–200 Ω/square. A principal limiting factor is concentration-enhanced diffusion of the base dopant [6]. Strained-layer GaInAs base regions have also been used, which may benefit from splitting of the light/heavy hole band degeneracy, as well as from increased electron velocity and greater emitter–base bandgap differences [7]. Fabrication approaches vary according to whether the base is contacted with the use of acceptor implantation and rapid thermal annealing, or by selective etching. In both cases, a major developmental goal is a "self-aligned" process in which the active emitter area and the edge of the base and emitter contacts are all defined with the same photoresist pattern, with controllably small (0.1 μm) separations between the regions. This reduces the area of the device which contributes parasitic base resistance and base–collector capacitance without contributing to transconductance. A number of self-aligned fabrication approaches have been reported recently [8]–[11]. Reactive ion etch-defined dielectric side walls and InGaAs top (emitter) contacting layers have been shown to

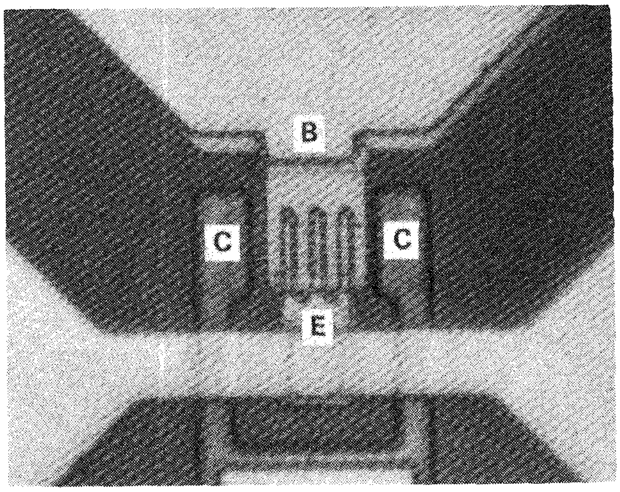

Fig. 3. Microphotograph of fabricated millimeter-wave HBT (with three emitter stripes of width 1.2 μm).

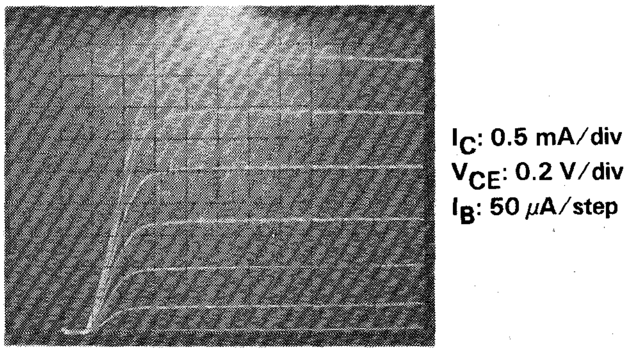

Fig. 4. Common-emitter $I-V$ characteristics of representative, high-speed HBT (emitter dimensions: 2 μm$\times$4.5 μm).

be useful techniques. An additional technique to minimize extrinsic base–collector capacitance is to compensate the collector region under the base contact with a damage implant (e.g., protons or oxygen).

Devices are fabricated on semi-insulating GaAs substrates and may be monolithically integrated, together with thin-film resistors and Schottky diodes, using conventional GaAs IC techniques.

As an example of present HBT technology, Fig. 3 shows a microphotograph of a millimeter-wave HBT fabricated at Rockwell with a self-aligned process based on selective etching and dielectric liftoff [3]. The emitter fingers are 1.2 μm$\times$9 μm; the structure was fabricated with conventional contact optical lithography.

IV. Device Characteristics

Fig. 4 illustrates representative HBT common-emitter dc $I-V$ characteristics. Transconductance increases with increasing collector current, reaching values of up to 5–10 mS/μm^2 of emitter area (corresponding to more than 10 000 mS/mm of emitter length with the above 1.2-μm-wide emitters). Structures operate with current densities up to 10^5 A/cm^2 without current gain or cutoff frequency falloff. The dc current gain h_{fe} is often a function of device size due to periphery recombination effects, although

(a)

(b)

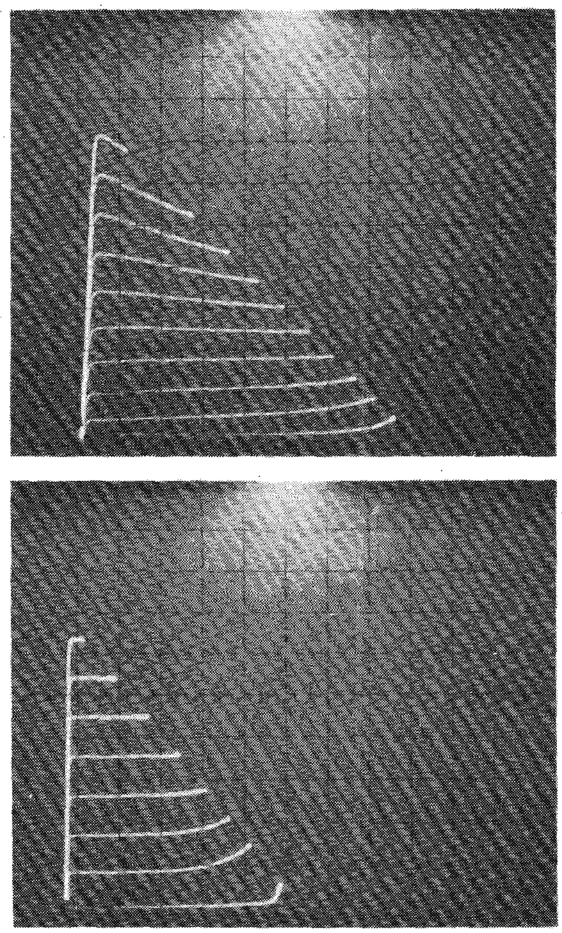

Fig. 5. $I-V$ characteristics in the high-voltage regime, showing breakdown. (a) Common-emitter characteristics (V_{ce}: 2 V/div, I_c: 1 mA/div, I_b: 50 μA/step). (b) Common-base characteristics (V_{cb}: 5 V/div, I_c: 0.5 mA/div, I_e: 0.5 mA/step).

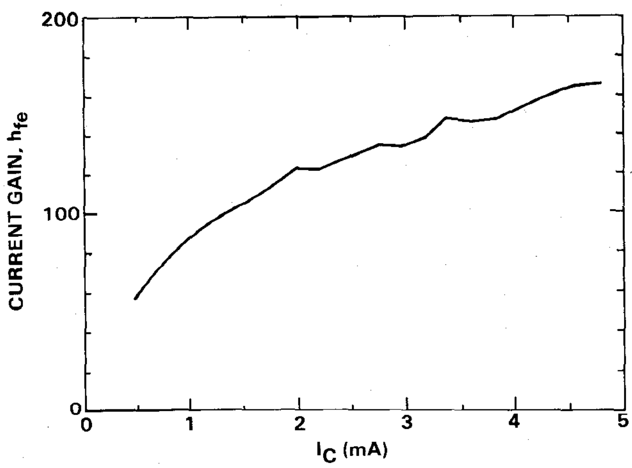

Fig. 6. Incremental dc current gain h_{fe} versus collector current for a 2 μm$\times$3.5 μm emitter device for digital and A/D applications.

these effects can be eliminated with graded bandgap bases [12] or appropriate AlGaAs edge passivation [13], [14]. Values in excess of 500 have been reached [15], although h_{fe} near 10–20 is commonplace in the fastest devices. Breakdown voltage is typically high: Fig. 5(a) and (b) shows $I-V$ characteristics on a high voltage scale for a

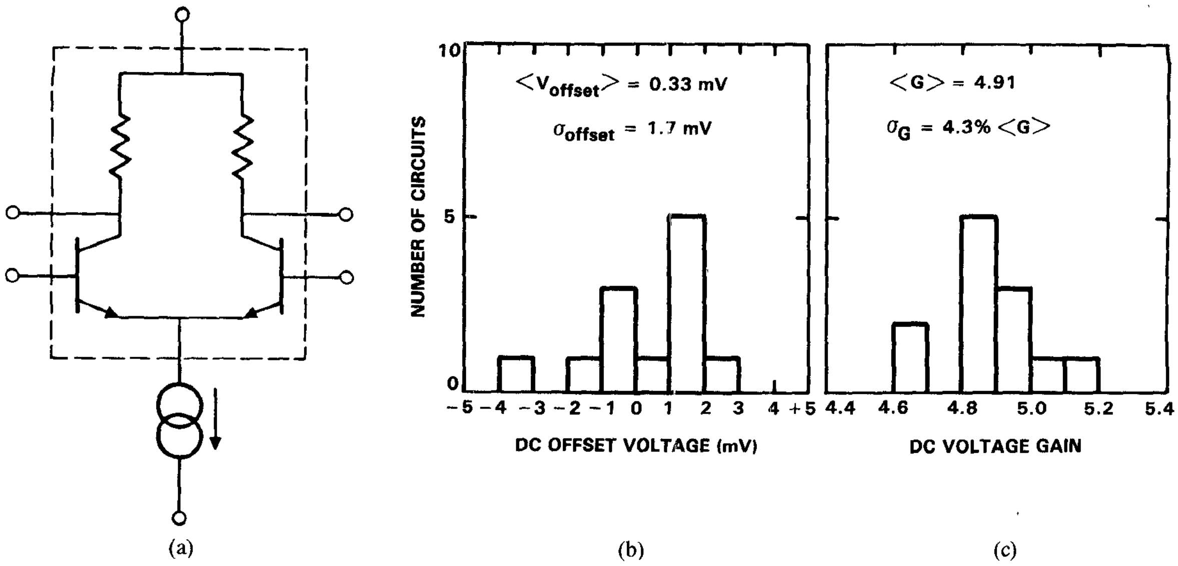

Fig. 7. (a) Prototype differential amplifier for device characterization. (b) Histogram of measured input offset voltages across a small wafer. (c) Histogram of corresponding voltage gain.

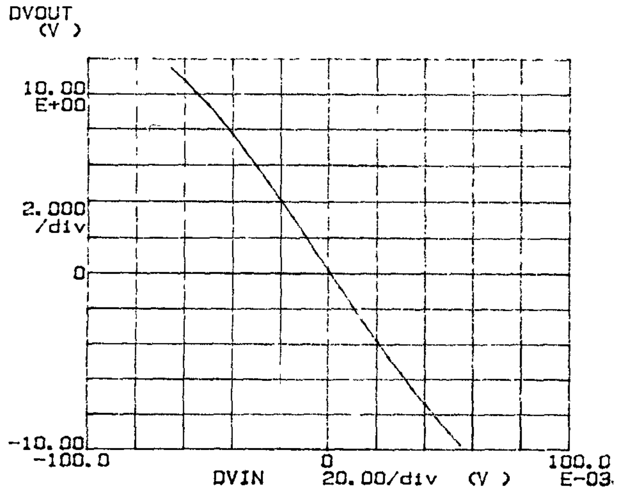

Fig. 8. Input–output voltage transfer curve for a single-stage differential amplifier showing gain of 200 (46 dB).

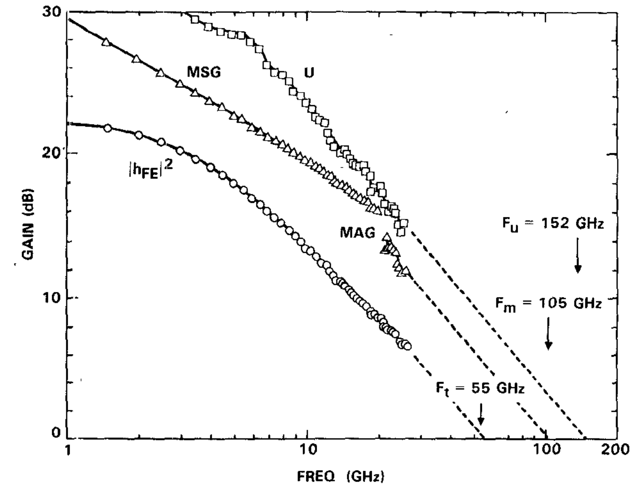

Fig. 9. Current gain h_{21} and power gain (*MSG*, *MAG*, and *U*) versus frequency, calculated from *S*-parameters measurements on a millimeter-wave HBT. Extrapolations to unity gain are shown at 6 dB/octave. *MAG*, maximum available gain, is shown above the frequency at which the device becomes unconditionally stable, and *MSG*, maximum stable gain, below that frequency. *U* is the unilateral gain or Mason invariant. The best estimate of f_{max} is believed to result from the extrapolation of *U* (indicated by f_U).

device with a 2.5 μm $\times$4.5 μm emitter in common-emitter and common-base operation, illustrating 15-V and 25-V breakdown voltages, respectively. In Fig. 5(a), the negative output conductance is noteworthy—it results from device heating and decreasing current gain with temperature. Apart from the thermal and possible interpad leakage effects, output conductance is negligible, due to the high base doping. Early voltages are typically well above 100 V.

For a variety of linear circuits, as well as analog-to-digital converters, high current gain (> 50) is desirable. Fig. 6 shows h_{fe} versus collector current for a Rockwell partially self-aligned device with 2 μm$\times$3.5 μm emitters. Values of dc current gain up to 170 are evident, despite the small device size. The matching of these devices is a critical issue for many applications. Prototype differential amplifiers, as shown in Fig. 7(a), distributed across an 18 mm$\times$18 mm wafer were measured. Fig. 7(b) and (c) shows histograms of the resulting input offset voltage and gain distributions, illustrating the excellent device matching obtained. A high voltage amplification factor is also evident if (external) high resistance loads are used. Fig. 8 shows input–output dc transfer curves for a single differential amplifier showing a voltage gain of 200 (46 dB).

Fig. 9 illustrates RF gain versus frequency as calculated from *S*-parameters measured with a Hewlett-Packard 8510 network analyzer coupled with a Cascade Microtech probe system. The transistor corresponds to the device of Fig. 3, biased at $I_c = 14$ mA and $V_{ce} = 1.4$ V. The current gain h_{21}, maximum available gain *MAG*, maximum stable gain *MSG*, and Mason unilateral gain *U* are shown, together

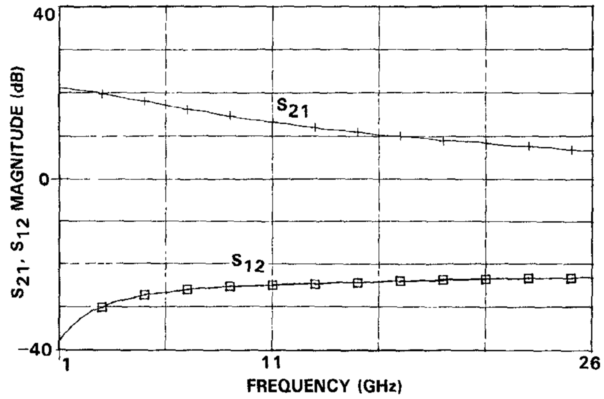

Fig. 10. Frequency dependence of the magnitudes of S_{21} and S_{12}, illustrating the highly unilateral nature of the device.

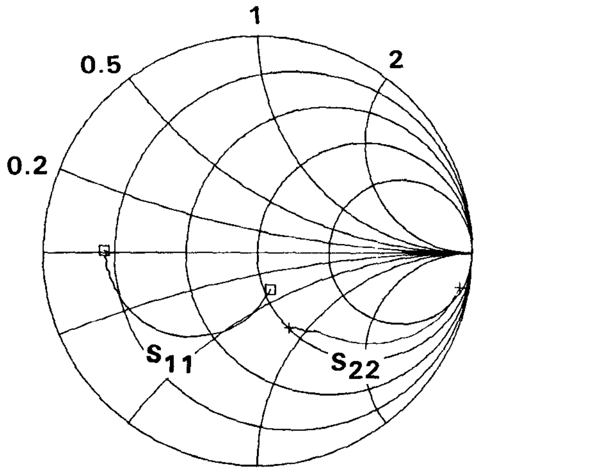

Fig. 11. Smith chart plot showing the variation with frequency of S_{11} and S_{22} (over the range 1–26 GHz).

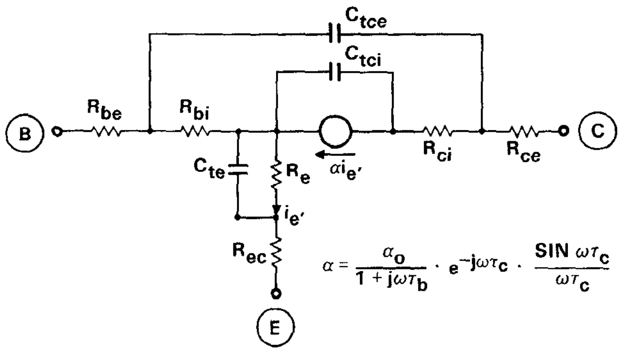

Fig 12. Approximate equivalent circuit of the HBT.

with the corresponding unity gain frequencies obtained by extrapolation of the data to higher frequency at 6 dB/octave. On theoretical grounds, *MAG* and *U* are expected to reach unity at the same frequency, the maximum frequency of oscillation $f_{\max}$. The data of Fig. 9 indicate that $f_{\max}$ for the HBT lies between 105 GHz and 152 GHz; simulation indicates further that the value is probably closer to the high end, inasmuch as *MAG* decreases with frequency f somewhat more slowly than $1/f^2$. Fig. 9 illustrates that HBT's can have useful gain well into the millimeter-wave frequency range (even with a

TABLE II
APPROXIMATE ELEMENT VALUES FOR LUMPED-ELEMENT CIRCUIT MODEL OF MILLIMETER-WAVE HBT

$\alpha_0 = 0.93$	$R_{be} = 4.6\,\Omega$
$\tau_b = 0.6$ ps	$R_{bi} = 1.7\,\Omega$
$\tau_c = 0.7$ ps	$R_e = 1.9\,\Omega$
$C_{te} = 0.7$ pF	$R_{ec} = 2.0\,\Omega$
$C_{tci} = 0.013$ pF	$R_{ce} = 3.0\,\Omega$
$C_{tce} = 0.026$ pF	$R_{ci} = 5\,3\,\Omega$

$I_c = 14$ mA; $V_{ce} = 1.4$ V.
Emitter dimensions: 1.2 μm$\times$9 μm (for each of 3 fingers).

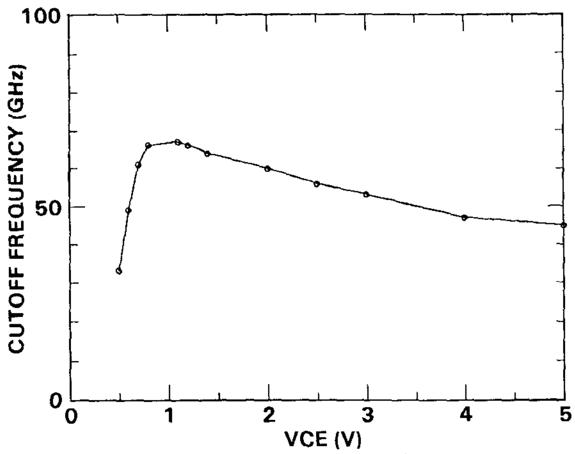

Fig. 13. Variation of cutoff frequency f_t with collector bias V_{ce}.

minimum geometry of 1.2 μm). As shown in Fig. 10, S_{21} is remarkably high and S_{12} remarkably low over the entire range of the data, so that the devices are easy to match and to cascade. Fig. 11 shows corresponding values of S_{11} and S_{22}. An approximate equivalent circuit for the device is illustrated in Fig. 12; Table II lists estimated values for the circuit elements in the model. The calculated current gain h_{21} shown in Fig. 9 extrapolates to a cutoff frequency f_t of 55 GHz. In separate devices, higher f_t values have been observed. Fig. 13 illustrates the measured dependence of f_t on V_{ce} in such a wafer. A maximum f_t of 70 GHz is obtained at $V_{ce} = 1$ V. With increasing V_{ce}, f_t drops due to the increased transit times of electrons across the base–collector depletion region. The value of f_t remains usefully high, however, over a wide region. Present record f_t performance corresponds to 105 GHz, achieved by NTT [16]. Simulations suggest $f_t = 150$ GHz is possible [17].

Several measurements have been made of HBT gain and power capabilities at frequencies above 26 GHz. In Fig. 14 is shown the measured gain versus input power for a device similar to that of Fig. 3 at 39 GHz for two different bias settings. The maximum gain was 10 dB, which extrapolates at 6 dB/octave to an $f_{\max}$ value of 123 GHz. At a separate bias (leading to lower gain), an output power of 30 mW was obtained, corresponding to a power density of 1 W per millimeter of emitter length. By comparison, a power density of 0.45 W per millimeter of gate width is the highest reported to date for GaAs MESFET structures at this frequency [18].

Extensive noise measurements have not yet been done on millimeter-wave HBT's. Based on early measurements

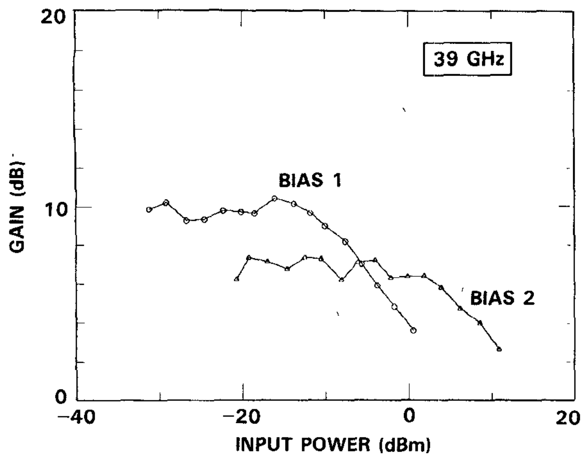

Fig. 14. Measured available gain versus input power level at 39 GHz for a millimeter-wave HBT at two bias settings. The highest gain corresponds to an extrapolated f_{max} of 120 GHz. The highest power corresponds to 1 W/mm of emitter length.

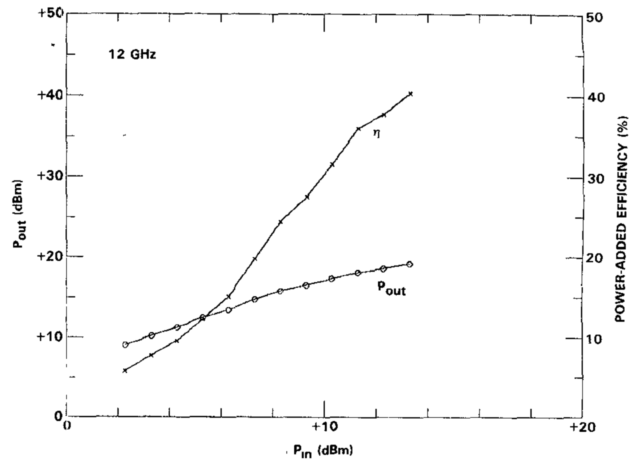

Fig. 15. Output power versus input power for a HBT with 2-μm emitter width at 12 GHz.

[19], it is believed that in the white noise regime, contributions from base current shot noise and base resistance Johnson noise are unlikely to allow noise figures to be competitive with state-of-the-art heterostructure FET's. In the $1/f$ noise regime, preliminary measurements [19] have shown noise corner frequencies below 1 MHz, a significant improvement over most FET's.

V. Integrated Circuit Prospects

The application of HBT's in microwave and millimeter-wave IC's is in its early infancy. For the most part, the applications are envisioned to follow paths established by Si bipolar technology, extended to considerably higher frequency. Some of the most promising areas include the following.

- Microwave power amplifiers of high efficiency. The high breakdown voltage and current handling capability of HBT's can lead to high power in small chip areas. Class B or Class C operation becomes convenient due to high gain and high breakdown voltage. The need for good heatsinking and possibly emitter ballasting are potential problems, although they are directly alleviated by pulsed operation. With discrete devices, initial demonstrations of common-base operation at 10 GHz have been done by Texas Instruments [20]. For CW operation, 4 W per mm of emitter length was obtained. A factor of two higher power density was demonstrated under pulsed operation. Similar results in common-emitter mode at 12 GHz have been achieved at Rockwell International. Fig. 15 illustrates the CW output power and power-added efficiency for an HBT with two emitter fingers of 10 μm length, as a function of input power. The efficiency reaches a value of 40 percent, a particularly high result.
- Wide-band analog circuits with frequency response from dc to 10 GHz. Use of feedback to obtain good control over gain and matching will be facilitated by high open-loop gain. As in lower frequency circuits, the inclusion of increasing numbers of active components and fewer large passive elements (inductors) will be favored. Low input offset voltages are available for dc coupling. Very good operational amplifiers should be possible. Nonlinear functions (AGC, log amps, multipliers, mixers) will be facilitated by the exponential input-voltage, output-current characteristics of HBT's.
- Millimeter-wave amplifiers, primarily power amplifiers. Projected f_{max} values are above 200 GHz, particularly with inverted structure HBT's with the collector on the wafer surface for reduced collector feedback capacitance [1]. The HBT is unique among candidate millimeter-wave devices in that it may be fabricated with conventional 1-μm optical lithography. Furthermore, HBT's are small enough that signal phase differences between different device regions are not a major concern, as they are for FET's.
- Microwave oscillators with low phase noise based on the relatively low $1/f$ noise associated with HBT's. Using discrete device, Agarwal has shown FM noise of −73 dBc/Hz at 1 kHz separation from the carrier with a dielectric resonator-stabilized oscillator at 4 GHz [21]. This FM noise value was 12 dB lower than the result obtained with a similar oscillator implemented with a GaAs FET.
- Analog/digital conversion. HBT's are particularly advantageous in the implementation of high-speed, high-accuracy comparators and flash converters due to their excellent input voltage matching, absence of hysteresis, and high speed [22]. HBT comparators have already been reported with offset error standard deviations on the order of 4 mV and 2.5 GSps operation [23]. The sensitivity of the comparators is consistent with resolution on the order of 8 bits, as illustrated by the data of Fig. 16 which depicts input and output waveforms for a HBT comparator during operation at 1 GSps, and a 3-mV Nyquist-limited (500 MHz) input. A 4-bit quantizer containing 16 HBT

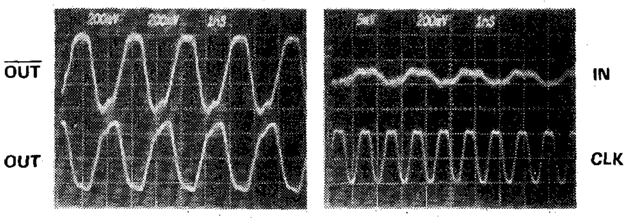

Fig. 16. Input and output waveforms for a HBT comparator illustrating 3-mV sensitivity at 1 GSps under Nyquist conditions (500 MHz input).

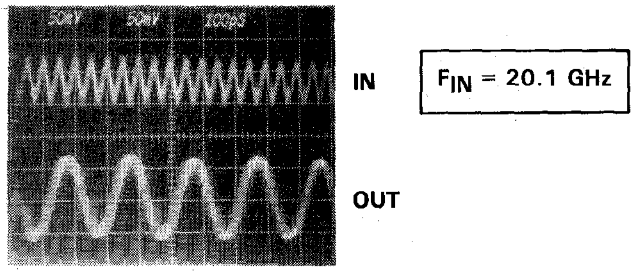

Fig. 17. Input and output waveforms for a HBT frequency divider ($\div 4$) operating above 20 GHz.

comparators and output encoding logic has been recently reported [24].

- Digital circuits. Digital techniques will be used in the future at frequencies heretofore considered exclusively analog. Frequency dividers are representative of maximum flip-flop toggling rate. With HBT's, static (master–slave) dividers have recently operated with above 20 GHz input frequencies [25]. Fig. 17 illustrates input and output waveforms for a divide-by-four circuit based on CML with 20.1 GHz input frequency. Power consumption per equivalent gate was 9 mW in this example. Recently, similar high-speed static frequency dividers (with 18-GHz operation) were reported for GaAs FET's. In that work, the FET gate length was 0.2 μm. In the HBT circuit, the emitter width was 2 μm, leading to more relaxed fabrication tolerances. Further increases in HBT digital circuit operating frequency appear feasible and millimeter-wave frequency dividers should be possible.

VI. Summary

HBT's have large amounts of current and power gain at microwave and millimeter-wave frequencies, and can be fabricated with straightforward optical lithography. Their current handling capability, input voltage dc matching, breakdown voltage, and $1/f$ noise are potentially better than those for GaAs FET's. Based on these characteristics, HBT's are expected to have a bright future in microwave/millimeter-wave IC's.

Acknowledgment

The authors are grateful to A. Gupta and B. Mathur for many helpful conversations and assistance in measurements, and to L. Sullivan for assistance in wafer growth.

References

[1] H. Kroemer, *Proc. IEEE*, vol. 70, p. 13, 1982.
[2] See, for example, R. N. Nottenburg, H. Temkin, M. B. Panish, R. Bhat, and J. C. Bischoff, *IEEE Electron. Device Lett.*, vol. EDL-7, p. 643, 1986; R. J. Malik, J. R. Hayes, F. Capasso, K. Alavi, and A. Y. Cho, *IEEE Electron. Device Lett.*, vol. EDL-4, p. 383, 1983; A. N. M. Masum Choudhury, K. Tabatabaie-Alavi, and C. G. Fonstad, *IEEE Electron Device Lett.* vol. EDL-5, p. 251, 1984; L. M. Su, N. Grote, R. Kaumanns, and H. Schroeter, *Appl. Phys. Lett.*, vol. 47, p. 28, 1985.
[3] See, for example, D. A. Sunderland and P. D. Dapkus, *IEEE Electron Device Lett.*, vol. EDL-7, 1986; and J. H. Hutchby, *IEEE Electron Device Lett.*, vol. EDL-7, p. 108, 1986.
[4] J. L. Lievin, C. Dubon-Chevallier, F. Alexandre, G. Leroux, J. Dangla, and D. Ankri, in *1985 Int. Symp. GaAs and Related Compounds* (Inst. Phys. Conf. Ser.), no. 79, 1986, p. 595.
[5] M. F. Chang, P. M. Asbeck, K. C. Wang, N. H. Sheng, G. J. Sullivan, and D. L. Miller, *IEEE Electron Device Lett.*, vol. EDL-8, p. 303, 1987.
[6] J. N. Miller, D. M. Collins and N. Moll, *Appl. Phys. Lett.*, vol. 46, p. 960, 1985.
[7] G. J. Sullivan, P. M. Asbeck, M. F. Chang, D. L. Miller, and K. C. Wang, *Electron. Lett.* vol. 22, p. 419, 1986.
[8] T. Izawa, T. Ishibashi, and T. Sugeta, in *Tech. Dig. 1985 IEDM*, p. 328.
[9] S. Tiwari, in *Tech. Dig. 1986 IEDM*, p. 262.
[10] N. Moll, in *Tech. Dig. 1985 Cornell Conf. Adv. Concepts in High Speed Dev. and Circuits.*
[11] M. F. Chang, P. M. Asbeck, D. L. Miller, and K. C. Wang, *IEEE Electron Device Lett.*, vol. EDL-7, p. 8, 1986.
[12] H. Ito and T. Ishibashi, in *1985 Int. Symp., GaAs and Related Compounds* (Inst. Phys. Conf. Ser.), no. 79, ch. 11, p. 607.
[13] H. H. Lin and S. C. Lee, *Appl. Phys. Lett.*, vol. 47, p. 839, 1985.
[14] S. Tiwari, *IEEE Trans. Electron Devices*, Feb. 1987.
[15] S. L. Su, W. G. Lyons, O. Tejayadi, R. Fischer, W. Kopp, H. Morkoc, W. McLevige, and H. T. Yuan, *Electron Lett.* vol. 19, p. 128, 1983.
[16] T. Ishibashi and Y. Yamauchi, presented at 1987 Dev. Res. Conf.
[17] K. Tomizawa, Y. Awano, and N. Hashizume, *IEEE Electron Device Lett.* vol. EDL-5, p. 362, 1984.
[18] B. Kim, H. M. Macksey, H. Q. Tserng, H. D. Shih, and N. Camilleri, *Microwave J.*, p. 153, Mar. 1987.
[19] P. M. Asbeck, A. K. Gupta, F. J. Ryan, D. L. Miller, R. J. Anderson, C. A. Liechti, and F. H. Eisen, in *Tech. Dig. 1984 IEDM*, p. 846.
[20] B. Bayraktaroglu, N. Camilleri, H. D. Shih, and H. Q. Tserng, in *Tech. Dig. 1987 IEEE MTT-S*, p. 969; see also B. Kim, H. Q. Tserng, S. K. Tiku, and H. D. Shih, *Electron Lett.*, vol. 21, p. 258, 1985.
[21] K. Agarwal, in *Tech. Dig. 1986 MTT-S*, p. 95.
[22] K. deGraaf and K. Fawcett, in *Tech. Dig. 1986 GaAs IC Symp.*, p. 205.
[23] K. C. Wang, P. M. Asbeck, M. F. Chang, D. L. Miller, and F. H. Eisen, in *Tech. Dig. 1985 GaAs IC Symp.*, p. 99.
[25] K. C. Wang, P. M. Asbeck, M. F. Chang, G. J. Sullivan, and D. L. Miller (to be published).
[26] J. F. Jensen, L. G. Salmon, D. S. Deakin, and M. J. Delaney, in *Tech. Dig. 1986 IEDM*, p. 476.

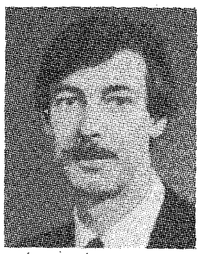

P. M. Asbeck (M'75) is a Member of the Technical Staff of the Heterostructure Bipolar Transistor Department at the Rockwell International Science Center. Dr. Asbeck attended MIT, where he received the B.S. and Ph.D. degrees in 1969 and 1975, respectively, both from the Electrical Engineering Department. His thesis research dealt with the preparation and physics of PbSe homojunction lasers.

Prior to joining Rockwell International, he worked at Philips Laboratories, Briarcliff Manor, NY, where he was concerned with the characterization, physics, and applications of (Ga, Al)/As/GaAs double heterostructure lasers. At Rockwell International Science Center, Dr. Asbeck has been involved in studies of ion implantation and related processing in GaAs, and with the development of III–V heterojunction devices. He investigated the diffusion of Cr in GaAs, and has studied the relationship between implant behavior and substrate characteristics. More recently, he has been active in the development of heterojunction bipolar transistors for use in digital and microwave circuits, and has contributed to the design, modeling, processing, and application of these devices.

Dr. Asbeck is a member of the American Physical Society.

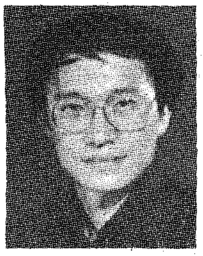

M. F. Chang (S'76–M'79) is a Member of the Technical Staff in the Heterostructure Bipolar Transistor Department of the Rockwell International Science Center. He received the B.S. degree in physics from National Taiwan University in 1972, the M.S. degree in Material Science from National Tsing-Hua University in 1974, and the Ph.D. degree in electrical engineering from National Chiao-Tung University in 1979. He joined the University of California at Los Angeles as a Post-Doctoral Fellow in 1979.

He was with Microwave Associate PHI in 1981 as a senior research and development engineer. He developed a fully ion-implanted process for high-power *L*-band and *S*-band Si bipolar transistors. After that, he joined TRW, Inc. in 1982 to conduct the development work on GaAs microwave IC's. He was also in charge of the GaAs technology transfer program from the TRW system division to the TRW semiconductor division. Since 1983, he has been at Rockwell International working on process development for GaAs IC's. In this position, Dr. Chang was responsible for the successful development of a self-aligned fabrication process for GaAs MESFET IC's and HEMT IC's. More recently, he has been instrumental in the development of improved processing techniques for heterojunction bipolar transistors for the past two years.

Dr. Chang is a member of the Phi-Tau-Phi Society.

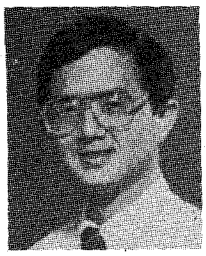

K.-C. Wang received the B.S. degree in physics from National Taiwan University in 1972 and the Ph.D. degree in physics from the California Institute of Technology in 1979. While at Caltech, he carried out studies on the energy dependence and natural line width of X-rays and relativistic splitting of energy levels in pionic atoms, using a high-precision bend crystal spectrometer.

He was a research physicist at the University of California, Irvine, from 1979 to 1985. During this period, he worked on neutrino electron scattering at Los Alamos National Lab and neutrino oscillations at Brookhaven National Lab. Dr Wang joined Rockwell International in March 1985, and is currently involved in the study of heterostructure bipolar transistors. He has been active in circuit and device modeling and circuit design and testing.

Dr. Wang is a member of the American Physical Society.

D. L. Miller received the A.B. degree in physics from Whitman College in 1966 and the M.S. and Ph.D. degrees in physics (1973) from the University of Illinois, Urbana.

Following his thesis work on excitonic superconductivity, he conducted research on superconductivity, surface physics, and amorphous silicon as a staff member at Brookhaven National Laboratories, Long Island, NY, from 1973 to 1977. Since joining Rockwell International, in 1977, he has been involved in using MBE for research on heterojunctions, polycrystal and single-crystal GaAs solar cells, cascade multijunction solar cells, GaAs FET's, and enhanced mobility modulation-doped GaAs/(Ga, Al)As material. Most recently, Dr. Miller has been involved in the investigation of high-speed heterojunction bipolar transistor technology using MBE material. He is presently manager of a department which includes heterojunction bipolar transistor research and development, MBE R&D, and GaAs IC processing support services.

Dr. Miller is a member of the American Physical Society and the American Vacuum Society.

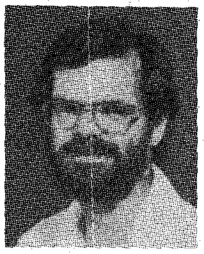

G. J. Sullivan is a Member of the Technical Staff in the Heterostructure Bipolar Transistor Department of the Rockwell International Science Center. He received the B.S. degree from St. Joseph's College in 1974, the M.S. degree from the University of Delaware in 1977, and the Ph.D. degree in electrical and computer engineering from the University of California at Santa Barbara in 1983. His Ph.D. dissertation studied the growth by MBE and electrical characterization of GaAs/Ge heterojunctions.

He has been employed at Rockwell (Anaheim) as a Silicon Process Engineer, at the Santa Barbara Research Center as an InSb Process Engineer, and at AT&T Bell Labs, Crawford Hill, fabricating and characterizing high speed, long-wavelength distributed feedback InGaAsP lasers. Dr. Sullivan is currently employed at Rockwell International, where he is involved in the development of heterostructure devices.

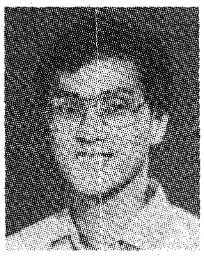

N. H. Sheng (S'80–M'86) is a Member of the Technical Staff in the Heterostructure FET Technology Department of the Rockwell International Science Center. Born in Taiwan, R.O.C. in 1952, he received the B.S. degree in electrical engineering from National Taiwan University in 1974 and the M.S. and Ph.D. degrees from the University of California at Santa Barbara in 1978 and 1982, respectively. His graduate research was on the electrically active defects in ion-implanted semiconductors after CW beam annealing using EBIC, PL, and DLTS techniques.

He joined Rockwell International in 1982 and worked on the process and device development of HgCdTe photovoltaic arrays, which led to the demonstration of high-performance HgCdTe focal plane arrays epitaxially grown on sapphire. Since 1983, he has been engaged in the development of HEMT devices and circuits.

E. Sovero (M'85) is a Member of the Technical Staff in the Heterostructure FET Technology Department at the Rockwell International Science Center. He obtained the Ph.D. degree in applied physics and information science from the California Institute of Technology in 1977. At Caltech, Dr. Sovero studied acoustic instabilities in rocket engines, acoustic noise generated by high-speed turbulent flames, and the thermodynamics and plasma chemistry of the glow discharge carbon dioxide lasers. In research conducted at the Jet Propulsion Labs, he studied the characteristics of the copper chloride laser (5100 Å) plasma using microwave diagnostic techniques.

Since joining Rockwell, he has worked developing tunable acousto-optic and electro-optic IR spectral filters. Since 1981, he has been involved in the modeling, design, and test of high-speed GaAs charge-coupled devices (CCD) used as building blocks of complex analog and optical signal processing functions. He is currently working in the development of HEMT transistor technology for use in millimeter-wavelength IC's (33 to 50 GHz).

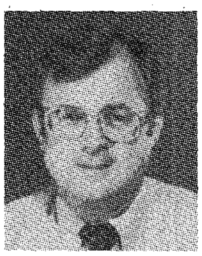

J. A. Higgins (M'62–SM'78) received the B.E. degree (Hons.) from Dublin University, Dublin, Ireland, in 1958, the M.S.E.E. degree from Stanford University, Stanford, CA, in 1964, and the Ph.D. degree in electrical engineering, also from Stanford University, in 1977.

He is presently Manager of the Millimeter-Wave Devices Department at Rockwell Science Center. Dr. Higgins joined Rockwell in 1971. From two years he was a leading member in the groups developing long-wavelength IR detector technology, which ultimately gave rise to a very successful focal plane technology. In 1973, he began to spearhead the development of the GaAs MESFET technology at Rockwell. This work, although initially aimed at providing a new generation of microwave devices, bore fruit in many directions, including the very successful digital MESFET IC's and the use of GaAs for a superior CCD for high-speed and optical applications. In the microwave area, Dr. Higgins's contributions were significant, for he pioneered the use of direct ion implantation into semi-insulating substrates as a means of obtaining the active layer for the devices. He led the way in the design of ultralinear power MESFET's through the first use of profile tailoring to obtain control over the onset of intermodulation products in these devices. In the area of circuit design, he was among the first to demonstrate the potential of the microwave monolithic IC by modeling and in using active matching on-chip. In 1980, Dr. Higgins took charge of the development of the GaAs CCD concept for high-speed applications. He is now Manager of all aspects of the application of these devices, which include signal processing, imaging, and electro-optical signal processing. In 1984, Dr. Higgins was placed in charge of a new activity to exploit the heterojunction technology transistors, which are: (1) high electron mobility transistors (HEMT's), and (2) heterojunction bipolar transistors (HBT's) for use in the millimeter-wave bands. To this end, he is assembling a new team from industry and colleges to push this project at a rapid place.

Dr. Higgins has authored or coauthored over 30 publications in the field of GaAs devices. He holds one patent in the area of microwave circuit design and has three more filed.